Clinical Characters in Pre-invasive and Invasive Adenocarcinoma with Pulmonary Ground-glass Nodules

han zheng (zhenghan395@tmu.edu.cn)
Tianjin Medical University https://orcid.org/0000-0002-5620-1384
Chongbiao Huang
Tianjin Medical University Cancer Institute and Hospital: Tianjin Tumor Hospital

Research Article

Keywords: ground-glass nodules (GGNs), pre-invasive adenocarcinoma, invasive adenocarcinoma (IAC), EGFR, PD-L1

Posted Date: November 30th, 2021

DOI: https://doi.org/10.21203/rs.3.rs-1101858/v1

Abstract

Purpose: With the increasing prevalence of pulmonary ground-glass nodules (GGNs) among younger population, its clinicopathologic performance, lung cancer-associated genetic mutation, and immune landscape features between pre-invasive adenocarcinoma and invasive adenocarcinoma (IAC) need to be get well known.

Methods: We retrospectively reviewed basic clinical information, analyzed radiological characteristics, and then evaluated the status of mutational hotspots and tumor mutational burden by sequencing genome in tissue. Programmed death ligand 1 (PD-L1) expression was detected by immunohistochemistry staining.

Results: Nodules vastly increased the probability of IAC when the diameter of GGNs was more than 1.15 mm or the consolidation-to-tumor ratio was at least 8.5%, with the latter predictor having a better diagnostic specificity. Tumors positive for exon 19 deletion and exon 21 L858R in EGFR mutation had a higher prevalence in IAC. However, there was no difference in PD-L1 expression. As expected, tumor mutational burden in IAC was higher, despite a low background mutational burden as a whole.

Conclusions: GGNs should be pay high attention when several aggressive behaviors showed in radiology and inner solid components increased gradually, providing more evidence apt to a diagnosis of IAC. We found that GGNs of IAC performed early genomic alternations events during the slow growth carcinogenesis stage of GGNs, including the most common proto-oncogene EGFR activation, which mainly concentrates on IAC. Indolent GGNs at an early stage usually have negative PD-L1 expression.

Introduction

The latest global cancer data shows that the incidence of lung cancer ranked second worldwide in 2020. In China, the incidence and mortality rank highest, constituting 23.8% of the total cancer deaths [1]. The extensive application of low-dose thoracic computed tomography (CT) in the detection of ground-glass nodules (GGNs) has increased, raising widespread attention in recent years. The GGNs are round-like or irregular ground-glass opacities, with cloudy fuzzy density shadows. The GGNs were observed in lung windows on CT, in which the internal blood vessels and bronchi were uncovered completely and often closely related to lung adenocarcinoma (LUAC). The GGNs are divided into pure GGN (pGGN) and mixed GGN (mGGN) based on differences in density. It is still a challenge diagnosing GGNs using radiology. Benign lesions are the leading cause of ground-glass changes, such as inflammatory infection, pulmonary fibrosis, granulomatous lesions, pulmonary haemorrhage, intrapulmonary lymph nodes, and carbon dust which could be contracted or absorbed gradually during long-term follow-up[2]. A small part of GGNs evolves into malignant tumors with slow growth in the early stage [3, 4]. Thus, proper management of these indolent GGNs is needed [5, 6]. Avoiding over-treatment and delayed surgery does not have a significant impact on prognosis[7, 8].

According to the recent WHO classification of thoracic tumors [9], adenocarcinoma in situ (AIS) was reclassified as precursor glandular lesion, with its management different from minimally invasive adenocarcinoma (MIA) and invasive adenocarcinoma (IAC), it was certainly worth taking into consideration because of molecular alterations[10, 11]. Wilshire et al. reported that disease-free survival (DFS) in AIS and MIA of lepidic adenocarcinomas in stage I could be 100% and 96% respectively and 80% in IAC after surgical resection. The overall survival in AIS and MIA was 100% more than in IAC, 90%. The GGNs of early LUAC possess better prognostic survival than solid nodules, especially pGGNs reaching nearly 100% DFS after resection[12–15]. In the early stages of LUAC, GGNs with unique biology still have their invasive behaviors from AIS/MIA to IAC. When nodules grew rapidly, solid components arose, or previous solid components increased during follow-up, the risk of developing IAC and invasiveness were relatively higher[16].

Preoperative evaluation of the radiological features of pulmonary GGNs and prediction of the degree of tumor infiltration can greatly help clinicians make diagnosis and treatment plans for malignant nodules. Knowing the dynamic genomic alterations and immune checkpoint status in pre-invasive and invasive LUAC could provide better guidance for precision-targeted therapy and immunotherapy in the latest treatments.

Materials And Methods

Patient Selection

We retrospectively reviewed complete electronic medical records of patients who accepted surgical resection of pulmonary GGNs at the Tianjin Medical University Cancer Institute and Hospital from March 2017 to May 2021. All eligible lesions met the following criteria; GGNs detected by CT and resected later, nodules confirmed with a pathologic result of AIS, MIA, and IAC. And lastly, specimen detected by next-generation sequencing. Patients were divided into two groups (AIS/MIA group and IAC group) according to the final pathological results of scope and degree of tumor cells infiltration.

Histopathologic Classification

After surgical resection, tissue specimens were used to make a histological examination of immunohistochemistry staining (IHC). Each lesion was classified as AIS, MIA, and IAC according to the WHO classification of lung adenocarcinoma. The growth pattern and range of invasion of cancer cells were observed under a light microscope. Senior pathologists made the final identification of pathologic subtypes.

Acquisition of Chest CT Images

Thoracic CT scans were performed in a 64-slice helical multidetector scanner (Optima CT680 Expert, USA) with multiple-plane reconstruction. Quantitative indexes were measured precisely using a pitch of 1.25mm in lung window settings (window level, 35 Hounsfield units [HU]; window width, 320 HU). Mixed

components in nodules were also observed to exclude calcification in the mediastinal window (window level, -500 HU; window width, 1200 HU). Meanwhile, the largest diameter was measured and analyzed when the lesion shapes were irregular or multiple lesions were present. Consolidation-to-tumor ratio (CTR) was defined as the ratio of the maximum size of the solid component against full lesion size in the axial plane (for pGGN, CTR=0; for mGGN, 0□CTR□1; for pure solid nodule, CTR=1). These images were evaluated for malignant performance combined with relative clinical information and history of past illness by two experienced radiologists.

Biomarker Detection

Sections of tumor tissue specimens were sent for next-generation sequencing in the Illumina sequencing platform. Comprehensive mutation information of the tumor tissues such as DNA point mutations, fusion, deletion, insertion, or germline mutation of lung cancer-relative hotspots were acquired using the GRCh37/hg19 genome as control. Subsequently, ALK-EML4, the most frequent fusion form, were evaluated by IHC with Ventana anti-ALK rabbit monoclonal primary antibody (D5F3, Roche). Not all patients admitted the detection of PD-L1 expression and tumor mutational burden (TMB) quantification in this study. In total, we collected 185 cases to assess the level of immune checkpoint PD-L1 expressed in tumor cells by Ventana PD-L1 Assay (SP263, Roche). According to the tumor proportion score (TPS), the results were marked as a negative or positive expression. The results could also be divided into low expression (1%-49%) and high expression (≥50%). In addition, TMB was defined as the number of somatic mutations per megabase of the analyzed genomic sequence and was detected in 228 patients by high throughput sequencing.

Statistical Analysis

Categorical variables were shown as numbers or percentages and compared by the Pearson chi-square test or Fisher exact test. Continuous variables were compared by directly applying the Mann-Whitney U Test, and values are described as mean ± standard deviation. Logistic regression analysis was performed to determine the relationship between potential risk predictors closely advancing into IAC. The receiver operating characteristic curve (ROC) was made, and the area under the curve (AUC) was calculated to identify a proper diagnostic index with its best cut-off of distinguishing nodules between the pre-invasive lesion and IAC. The statistical analyses were done using SPSS software (version 26.0, IBM Corp, Armonk, NY) and GraphPad Prism software (version 8.0, GraphPad Software, La Jolla, CA). Tables and figures were generated using Microsoft Office 2019 (Microsoft, Redmond, WDC, USA). Inspection levels $\alpha = 0.05$ were considered statistically significant when the p-value was less than 0.05.

Results

Clinicopathologic Characteristics

378 GGNs from 328 patients (287 cases of single nodules and 41 cases of multiple nodules) were analyzed. There were 224 GGNs (59.2%) of IAC, 26 (6.9%) of AIS, and 128 (33.9%) of MIA. The majority

were females, 222 (67.7%) out of which 211 cases had no smoking history. The males were 106 (32.3%), with only 33 nonsmokers. These patients had a median age of 57 years (age range, 31-76 years, 56.29±9.85), which could be present in three grades (< 45 years for 12.8%, 45≤age≤65 years for 69.5%, >65 years for 17.7%). As expected, nodules were almost located at bilateral upper lobe (246/378, for 65.1%), lower lobes also were common area for 26.7%, while middle lobe only had 31 lesions (for 8.2%). Patients without lymph node metastasis were 323 (98.5%), out of which 5 (1.5%) of IAC lymph nodes were positive. Patients with clinical stages IA (69.8%) and IB (24.4%) were the leading, accounting for 94.2%, Stage IIA were 2 (0.6%), 5 (1.5%) in stage IIB, and 1 (0.3%) in stage IIIA (Table 1).

GGNs of IAC had More Aggressive Performance in Radiological Characteristics

Approximately 134 (35.4%) pGGNs and 20 (5.3%) mGGNs were identified as AIS/MIA, while 96 (25.4%) pGGNs and 128 (33.9%) mGGNs were identified as IAC. The mean nodules diameter of the AIS/MIA was nearly one-half of the diameter of IAC (0.92±0.029 versus 1.77±0.049 [p<0.001]) (Fig.1a). Compared to the solid inner component, the mean CTR was approximately four times higher in AIS/MIA than in IAC (0.57±0.033 versus 0.13±0.027 [p<0.001]) (Fig.1b). GGNs of two subtypes had their morphological performance on CT(Fig.2). Most GGNs were round. The IAC irregular nodules were, 97 (25.7%) while AIS/MIA were 7 (1.8%) (p<0.001). The AIC and AIS/MIA nodules had an indistinct bound with a percentage of 21.9% and 40% (p=0.008), respectively. Vessel gather, air bronchogram, and pleural traction in IAC were 23%, 18%, and 28.6% respectively and 2.9%, 3.2%, and 4.2% respectively in AIS/MIA (p<0.001). It was observed that GGNs lobulation and bubble lucency were higher in IAC (34.4% and 39.1%) than in AIS/MIA (4% and 10.6%) (p<0.001). Although GGNs with a spicule sign were rare, 12.2% were detected in IAC and 0.8% in AIS/MIA. Among these basic indexes and unfavorable signs displayed in radiological images, the location of nodules had no influence (p=0.72). Nodule size, consolidation tumor ratio, lobulation, spicule sign, vessel gather, air bronchogram, pleural traction, and bubble lucency were significantly different between AIS/MIA and IAC with its contribution values <0.05 (Table 2).

These meaningful univariate features were analyzed using multivariate indexes in logistic regression. Size of nodule, CTR, lobulation, as well as pleural traction were proven to be independent risk predictors that affect GGNs being IAC (p<0.05) (Table 3). The highest AUC was 0.73 (95% CI, 0.68-0.96) when CTR was 8.5%, with its sensitivity of 57.1% and specificity of 87%. The AUC in a diameter of 1.15 cm nodule was 0.87 (95% CI, 0.84-0.91) with its sensitivity 81.3% and specificity 78.6%, both of which had significant differences (p<0.001, Fig.3).

EGFR-mutated Invasive Adenocarcinoma Played Predominant Role in GGNs

About 332 lesions from 378 GGNs had their genomic profiles with multiple driver gene site mutations. The lesions include 121 AIS/MIA and 211 IAC (Fig.4a). The wild genotype of the relative gene was detected in 25 lesions. Mutation of gene EGFR was the most frequent, accounting for 216 (65.1%) GGNs, including 165 (76.4%) IAC and 51 (23.6%) AIS/MIA (Fig.4b). Patients of EGFR mutations were more likely to be IAC 78.2% than EGFR- wild type 38% ($p<0.001$). Exon19 deletion and exon 21 L858R were the predominant site changes accounting for 67 (20.18%) and 117 (35.24%) respectively. The site changes in IAC, exon 19 deletions were 26.5% and exon 21 L858R were 43.6%; while in AIS/MIA, exon 19 deletions were 9.1% and exon 21 L858R 20.7%, both of two mutations made sense ($p<0.001$). There were 14 lesions with exon 20 mutation, including two T790M mutations in AIS/MIA and IAC, respectively. The AIS/MIA was more likely to change in exon 20 7.4% than IAC 2.4% ($p=0.027$). Mutation in exon18 was not statistically significant as it was less common (5% AIS/MIA versus 3.3% IAC $p=0.654$) (Fig.4c). In mGGNs, exon 20 mutation of IAC were 5/5 (100%), more than AIS/MIA 2/9 (22.2%) ($p=0.05$). Likewise, exon 21 L858R of EGFR of IAC were 59/92 (64.1%), more than AIS/MIA 4/25 (16%) ($p<0.001$). There were no significant differences in exon18 or exon19 of EGFR mutations (Fig.4d).

There were two EML4-ALK fusion mutations from six ALK mutations in AIS/MIA and IAC, respectively. The three ROS1-mutated patients with one positive fusion mutation belonged to IAC. Only one specimen had BRAF V600E mutation in 20 BRAF-mutated patients (Fig.4e). Thirty patients had HER2 mutation, out of which 22 were in AIS/MIA. About 22 specimens had KRAS mutation, of which 9 were AIS/MIA and 13 IAC, with two having both EGFR L858R and TP53 inactivation. About 44 patients had the tumor-suppressor gene (TSG) TP53 inactivation, followed by other gene mutations. Among 35 patients with TP53 mutation carried by EGFR mutation, four patients were AIS/MIA, and 31 were IAC (Fig.4f). Eight IAC positive specimens had one exon 14 skipping mutation and one gene amplification. Three of the six specimens had RET mutation with EGFR L858R mutation, and the other fused with CCDC6□KIF5B, and NTRK3. Amplification of MDM2 was observed in 11 specimens, of which seven were IAC. Gene fusion of NTRK1/2/3 could also be seen in 10 specimens, of which 7 were IAC. In addition, other gene mutations of PIK3CA, MAP2K1, and CDKN2A are detailed in Figure 4b.

Immune-relative landscape Feature Analysis

We evaluated the expression of PD-L1 in 185 patients (67 AIS/MIA and 118 IAC) and (109 pGGNs and 76 mGGNs). Sixty-seven expressed PD-L1, while 118 were negative. Twenty-two (32.8%) of the PD-L1 positives were AIS/MIA and 45 (38.1%) IAC ($p=0.471$) (Fig.5a). Neither GGNs in the negative PD-L1 expression nor in two level positive expression, there were no difference of between AIS/MIA and IAC(Fig.5b). Among the distribution of three expression levels of PD-L1 accompanied with diverse driver gene mutations, negative PD-L1 expression with EGFR-mutated GGNs were the predominant part, followed with low PD-L1 expression with EGFR-mutated GGNs, and those small part of high PD-L1 expression GGNs mainly had EGFR mutation (Fig.5c).

In addition, 228 specimens (83 AIS/MIA and 145 IAC) were sequenced for tumor mutational burden. The mean mutational base in AIS/MIA of GGN patients was significantly lower than in IAC (3.14±0.42 and 3.62±0.34 respectively, [p=0.041]) (Fig.1c).

Discussion

The pulmonary GGNs could be detected without any symptoms during regular health examinations[17]. Although GGNs can grows in any part of the lung, they mostly reside in the bilateral upper lobes, especially in the right lung. According to Chen et al., the prevalence of lung cancer among people older than 45 years increases significantly with age[18]. This report agrees with the findings of the present study; we found that patients aged 45 to 65 years had a higher risk of developing GGNs in LUAC, which was more common in female non-smokers. The GGNs have been identified as a signal of potential early LUAC. Unlike solid adenocarcinoma (SADC), GGNs had satisfactory prognoses of long-term OS in apparent characteristics of indolent growth and rare lymph node metastasis, including distant metastasis and inner changes of cancer cells and tumor microenvironment (TME) [19]. Liu et al. found that the prognosis in patients with IAC is worse than in AIS/MIA; the five-year DFS in patients with AIS/MIA was 100% and 74.1% in IAC[20]. Notably, GGNs smaller than 6 mm or stable for five years still had a risk of developing LUAC[21, 22]. Clinical management, taking measures, and continued follow-up mainly relied on morphological characteristics and behavior of GGNs[23]. It is worth noting that an unfavorable location such as hilus pulmonis might influence disease progression and accelerate early intrapulmonary lymph node metastasis, as was observed in this study.

Early growth of the tumor is accompanied by neovascularization and vascular remodeling. Localized or extensive tumor cells typically infiltrate, invade the surrounding lung tissue, and fibrous tissue proliferates with shrinkage, stretching the adjacent visceral pleura, along with hyperplasia of alveolar epithelial and thickening of the alveolar septum[24–26]. Before tumor histopathological diagnosis is made, objective quantitative indicators of the maximum diameter and solid component of GGNs could effectively evaluate the degree of invasion in LUAC[27]. The larger size of GGNs, the greater risk of malignancy. The solid component is representative of mGGNs, as its appearance showed a higher possibility of IAC. The transformation from pGGN into mGGN is more likely to a process of tumor-advanced evolution from AIS into IAC with a gradual increase in the proportion of solid components. The invasiveness improves until a complete solid nodule with strong invasiveness is achieved. Research has shown that, unlike SADC, GGNs of LUAC are characterized by slow growth, low-grade malignancy, and downregulation of signaling pathways related to cell proliferation and angiogenesis at the molecular level[19]. Molecular alterations, biological characteristics, and clinical phenotypes of GGNs are also affected by intratumor heterogeneity (ITH), as oncogenic drivers of all tumor cells within the same primary tumor may be different[28–30].

Herein, EGFR was the most frequent driver for gene mutation, with exon 21 L858R mutation being the most prevalent, followed by exon 19 deletion. These findings concur with previous pandemic statistics[31, 32], considering cancer-promoting genes in tumor genesis and processing[33]. Subtle alterations emerged

in EGFR status as a tumor at an early stage of AIS was seen in the case of one AIS patient of pGGN with EGFR L858R- positive mutation. Besides, HER2, BRAF, KRAS, and MAP2K1 mutations were also seen in pre-invasive lesions, suggesting that multiple gene activation might induce early stage tumorigenesis. A study reported that mutations in the canonical cancer genes, EGFR, HER2, NRAS, and BRAF, participate in early genomic events before the acquisition of invasiveness[10]. However, another study reported no significant difference in EGFR mutation alteration between early and advanced cancer stages[34], suggesting that EGFR mutation participates in tumor initiation and maintenance. A systematic review reported that EGFR mutation in GGNs had no apparent relationships in neither radiological progression nor tumor advancement[35]. On the contrary, we found that the frequency of EGFR mutations in IAC was more than AIS/MIA. We, therefore, hypothesized that some special components were generated to promote tumor progress by positive feedback during the slow-growing phase of GGNs. Later we found that mGGNs were the predominant type in IAC patients with positive EGFR mutation, causing us to pay closer attention to solid components that could influence tumor invasiveness. The Solid component showed pathological changes, including increased fibrotic tissue, vastly infiltrated tumor cells, and angiogenesis, providing a comfortable TME for a variety of tumor-associated cells and promoting tumor growth as well as a malignant biological behavior. To some extent, early complex TME with high ITH attributed to different phenotypes and invasion of LUAC with EGFR mutation[36]. Surprisingly, researchers have a strong interest in predicting EGFR mutation status in a non-invasive method with CT images, though it had not been sufficiently explored[37].

Besides, the status of ALK rearrangement was also crucial among LUAC. Patients with stage IA of ALK-positive adenocarcinoma had a worse prognosis and higher chances of developing regional lymph node metastasis[38]. Whereas ALK-positive mutation is common in GGNs, his study recorded only two in six patients with ALK fusion mutations, and no ALK fusion co-existed with any other mutation. However, this result could be attributed to the few samples examined in the present study. Similar findings were recorded in other genetic markers. TP53 as a co-existing gene mutation in LUAC with GGNs played a crucial role in maintaining normal cell growth and inhibiting tumor proliferation, of which inactivation could promote carcinogenesis and cancer metastasis. A previous study reported that TP53 mutation could disrupt the regular cell cycle control, becoming an early tumor-initiating event in EGFR-mutant LUAC[28]. Herein, we found 16.2% EGFR-mutant patients with TP53 mutation, which is less than a previous study that reported 30–60% mutation[39]. Xu et al. found that TP53 mutation could significantly affect the sensitivity of tumor cells to EGFR-TKI and long-term prognosis, resulting in primary resistance[40]. Besides, TP53 was thought to have an association with germline mutations in LUAC[41]. Since the solid component of GGNs was less than that of nodules and had lower invasiveness, we speculate that TP53 mutation in GGNs was unfavorable and might reduce the efficacy of targeted therapy of EGFR.

The expression of PD-L1 in tumor tissues was up-regulated to escape immune response due to acquiring resistance to molecular targeted therapy[42]. As such, immunotherapy compensates for wild-type driver genes and disease progression, achieving significant clinical benefits[43–46]. In the present study, the

expression level of PD-L1 positively correlated with the therapeutic effect; the higher the TPS, the greater the clinical benefit[46, 47]. Following previous studies, the PD-L1 expression was pretty lower in GGNs, predicting that GGNs had their unique immune mechanism and patients may have a less sensitive response to PD-L1 inhibitors than SADC[35, 48]. D.P. Carbone et al. reported that patients with PD-L1 ≥5% and a higher TMB level respond better to immunotherapy[49]. Another study proposed that EGFR-mutated patients with primary resistance might benefit from immunotherapy if both PD-L1 and $CD8^+$ are positive[50]. Notably, high PD-L1 expression was found when TP53 mutation was without co-occurring gene alterations[51]. The study found that pathological subtypes in GGNs do not influence the expression of PD-L1 in tumor cells. In contrast, PD-L1-negative patients also benefited significantly, making the benefit group no longer limited to PD-L1-positive patients[52].

The present study revealed that changes in TMB appear in the early stage of lesions. Notably, IAC patients had a higher TMB, suggesting that an activation pathway accelerated gene mutation in IAC even if GGNs had a low mutational burden. TMB played a predictive effect on immunotherapy since somatic mutations could produce new antigens and then be recognized by T cells to kill tumor cells[53–55].

In fact, some shortcomings of this study, such as manual measurement of the nodule diameter, and subjective judgment of CT signs, might cause deviations in the research findings to a certain extent, and reflecting the clinical-pathological characteristics of GGNs in an unprecise way. Limiting to a small sample size, the result could not represent overall data well. On the other hand, tumors had ITH not only in multifocal lesions, but in different region of the same nodule, small tissue specimens could not provide complete information about genetic alterations in GGNs. Last but not the least, we did not conduct the whole exome sequencing in those tumor tissue specimens, and the thorough molecular mechanism behind slow growth of GGNs was not refer to. All of these limitations mentioned above will be take into consideration in further exploration.

Conclusion

In summary, the sluggish growth of GGNs usually have a safe follow-up period. Surgical intervention should be timely when the nodules grow, new solid components create, or typical malignant signs of lobulation, spicule sign, and pleural traction are showed on CT, which are considered as reflections of IAC possibly. Besides size of nodules, the index CTR is a more favorable predictor to distinguish IAC from GGNs. There must be some special single pathways activated to modify the growth pattern of GGNs, different from the mechanism in SADC. Early events of genetic alterations like EGFR, KRAS, TP53 mutations emerge to regulate the tumorigenesis and advance. Consistent with most LUAC, proto-oncogene EGFR activation is the most frequent mutation in GGNs of IAC. In addition, we reveal that most GGNs have negative expression of PD-L1, indicating immunological escape does not play a predominant role in tumorigenesis at the early stage. Though low mutational burden in GGNs, we do not sure whether those patients are sensitive to immunotherapy or not. In general, patients with pulmonary GGNs of LUAC

often have a preferable prognosis and survival and EGFR-mutated patients may benefit a lot from molecular targeted adjuvant therapy.

Abbreviations

adenocarcinoma in situ (AIS); area under the curve (AUC); computed tomography (CT); consolidation-to-tumor ratio (CTR); disease-free survival (DFS); ground-glass nodules (GGNs); intratumor heterogeneity (ITH); immunohistochemistry staining (IHC); invasive adenocarcinoma (IAC); lung adenocarcinoma (LUAC); minimally invasive adenocarcinoma (MIA); mixed GGN (mGGN); programmed death ligand 1 (PD-L1); pure GGN (pGGN); receiver operating characteristic curve (ROC); solid adenocarcinoma (SADC); tumor microenvironment (TME); tumor mutational burden (TMB); tumor proportion score (TPS).

Declarations

Funding:

This work was supported by the project of the scientific research plan of Tianjin Educational Commission, China (2018ZD04).

Competing Interests:

The authors have no relevant financial or non-financial interests to disclose.

Author Contributions:

Conceptualization, Chongbiao Huang; methodology, Chongbiao Huang; validation, Chongbiao Huang; formal analysis, Han Zheng; investigation, Chongbiao Huang; data curation, Han Zheng; writing—original draft preparation, Han Zheng; writing—review and editing, Chongbiao Huang; visualization, Chongbiao Huang; supervision, Chongbiao Huang; project administration, Chongbiao Huang; funding acquisition, Chongbiao Huang. All authors have read and agreed to the published version of the manuscript.

Ethics approval:

This is a retrospective study. The Ethics Committee of Tianjin Medical University Cancer Institute and Hospital has confirmed that no ethical approval is required.

Consent to participate:

Informed consent was obtained from all individual participants included in the study.

Consent to publish:

The authors affirm that human research participants provided informed consent for publication of the images in Figure 2.

Acknowledgments:

We thank medical workers of Senior Ward in Tianjin Medical University Cancer Institute and Hospital for their support to this work.

References

1. SUNG H, FERLAY J, SIEGEL RL et al (2021) Global Cancer Statistics 2020: GLOBOCAN Estimates of Incidence and Mortality Worldwide for 36 Cancers in 185 Countries [J]. CA Cancer J Clin 71(3):209–249
2. OH J Y, KWON S Y, YOON H I et al (2007) Clinical significance of a solitary ground-glass opacity (GGO) lesion of the lung detected by chest CT [J]. Lung Cancer 55(1):67–73
3. LEE S W, LEEM C S, KIM T J et al (2013) The long-term course of ground-glass opacities detected on thin-section computed tomography [J]. Respir Med 107(6):904–910
4. QI L, XUE K, LI C et al (2019) Analysis of CT morphologic features and attenuation for differentiating among transient lesions, atypical adenomatous hyperplasia, adenocarcinoma in situ, minimally invasive and invasive adenocarcinoma presenting as pure ground-glass nodules [J]. Sci Rep 9(1):14586
5. HATTORI A, SUZUKI K, TAKAMOCHI K et al (2021) Prognostic impact of a ground-glass opacity component in clinical stage IA non-small cell lung cancer [J]. J Thorac Cardiovasc Surg 161(4):1469–1480
6. ZHANG Y, FU F (2020) Management of Ground-Glass Opacities in the Lung Cancer Spectrum [J]. Ann Thorac Surg 110(6):1796–1804
7. LI Q, MD J D, PENG Z M et al (2021) Management of Pulmonary Ground Glass Nodules: Less Is More [J]. The Annals of Thoracic Surgery
8. NAIDICH D, BANKIER A, MACMAHON H et al (2013) Recommendations for the management of subsolid pulmonary nodules detected at CT: a statement from the Fleischner Society [J]. Radiology 266(1):304–317
9. TRAVIS W D BRAMBILLAE, NICHOLSON A G et al (2015) The 2015 World Health Organization Classification of Lung Tumors: Impact of Genetic, Clinical and Radiologic Advances Since the 2004 Classification [J]. J Thorac Oncol 10(9):1243–1260

10. ZHANG C, ZHANG J, XU F P et al (2019) Genomic Landscape and Immune Microenvironment Features of Preinvasive and Early Invasive Lung Adenocarcinoma [J]. J Thorac Oncol 14(11):1912–1923
11. CHEN H, CARROT-ZHANG J, ZHAO Y et al (2019) Genomic and immune profiling of pre-invasive lung adenocarcinoma [J]. Nat Commun 10(1):5472
12. WILSHIRE C, L, LOUIE B E, HORTON M P et al (2016) Comparison of outcomes for patients with lepidic pulmonary adenocarcinoma defined by 2 staging systems: A North American experience [J]. J Thorac Cardiovasc Surg 151(6):1561–1568
13. HATTORI A, HIRAYAMA S, MATSUNAGA T et al (2019) Distinct Clinicopathologic Characteristics and Prognosis Based on the Presence of Ground Glass Opacity Component in Clinical Stage IA Lung Adenocarcinoma [J]. J Thorac Oncol 14(2):265–275
14. FU F, ZHANG Y, WEN Z et al (2019) Distinct Prognostic Factors in Patients with Stage I Non-Small Cell Lung Cancer with Radiologic Part-Solid or Solid Lesions [J]. J Thorac Oncol 14(12):2133–2142
15. YE T, DENG L, WANG S et al (2019) Lung Adenocarcinomas Manifesting as Radiological Part-Solid Nodules Define a Special Clinical Subtype [J]. J Thorac Oncol 14(4):617–627
16. KIM Y W, LEE C T (2019) Optimal management of pulmonary ground-glass opacity nodules [J]. Transl Lung Cancer Res 8(Suppl 4):S418–SS24
17. ZHANG Y, JHEON S, LI H et al (2020) Results of low-dose computed tomography as a regular health examination among Chinese hospital employees [J]. J Thorac Cardiovasc Surg 160(3):824–831e4
18. CHEN W, ZHENG R, BAADE PD et al (2016) Cancer statistics in China, 2015 [J]. CA Cancer J Clin 66(2):115–132
19. LU T, YANG X, SHI Y et al (2020) Single-cell transcriptome atlas of lung adenocarcinoma featured with ground glass nodules [J]. Cell Discov 6:69
20. LIU S, WANG R, ZHANG Y et al (2016) Precise Diagnosis of Intraoperative Frozen Section Is an Effective Method to Guide Resection Strategy for Peripheral Small-Sized Lung Adenocarcinoma [J]. J Clin Oncol 34(4):307–313
21. KOBAYASHI Y, FUKUI T, ITO S et al (2013) How long should small lung lesions of ground-glass opacity be followed? [J]. J Thorac Oncol 8(3):309–314
22. LEE H W, JIN K N LEEJK et al (2019) Long-Term Follow-Up of Ground-Glass Nodules After 5 Years of Stability [J]. J Thorac Oncol 14(8):1370–1377
23. MACMAHON H, NAIDICH D, GOO J et al (2017) Guidelines for Management of Incidental Pulmonary Nodules Detected on CT Images: From the Fleischner Society 2017 [J]. Radiology 284(1):228–243
24. WEICHERT W (2014) Early lung cancer with lepidic pattern: adenocarcinoma in situ, minimally invasive adenocarcinoma, and lepidic predominant adenocarcinoma [J]. Curr Opin Pulm Med 20(4):309–316
25. GAO JW, MA L H RIZZOS et al (2017) Pulmonary ground-glass opacity: computed tomography features, histopathology and molecular pathology [J]. Transl Lung Cancer Res 6(1):68–75

26. GAO F, SUN Y, ZHANG G et al (2019) CT characterization of different pathological types of subcentimeter pulmonary ground-glass nodular lesions [J]. Br J Radiol 92(1094):20180204
27. KAKINUMA R, NOGUCHI M, ASHIZAWA K et al (2016) Natural History of Pulmonary Subsolid Nodules: A Prospective Multicenter Study [J]. J Thorac Oncol 11(7):1012–1028
28. NAHAR R, ZHAI W, ZHANG T et al (2018) Elucidating the genomic architecture of Asian EGFR-mutant lung adenocarcinoma through multi-region exome sequencing [J]. Nat Commun 9(1):216
29. CROCKFORD A, JAMAL-HANJANI M, HICKS J et al (2014) Implications of intratumour heterogeneity for treatment stratification [J]. J Pathol 232(2):264–273
30. CAI W, LIN D, WU C et al (2015) Intratumoral Heterogeneity of ALK-Rearranged and ALK/EGFR Coaltered Lung Adenocarcinoma [J]. J Clin Oncol 33(32):3701–3709
31. SHIGEMATSU H, LIN L, TAKAHASHI T et al (2005) Clinical and biological features associated with epidermal growth factor receptor gene mutations in lung cancers [J]. J Natl Cancer Inst 97(5):339–346
32. BAEK J H, SUN J M, MIN Y J et al (2015) Efficacy of EGFR tyrosine kinase inhibitors in patients with EGFR-mutated non-small cell lung cancer except both exon 19 deletion and exon 21 L858R: a retrospective analysis in Korea [J]. Lung Cancer 87(2):148–154
33. SUN F, XI J, ZHAN C et al (2018) Ground glass opacities: Imaging, pathology, and gene mutations [J]. J Thorac Cardiovasc Surg 156(2):808–813
34. PI C, XU C R, ZHANG M F et al (2018) EGFR mutations in early-stage and advanced-stage lung adenocarcinoma: Analysis based on large-scale data from China [J]. Thorac Cancer 9(7):814–819
35. WEI Z, WANG Z, NIE Y et al (2021) Molecular Alterations in Lung Adenocarcinoma With Ground-Glass Nodules: A Systematic Review and Meta-Analysis [J]. Front Oncol 11:724692
36. HE D, WANG D, LU P et al (2021) Single-cell RNA sequencing reveals heterogeneous tumor and immune cell populations in early-stage lung adenocarcinomas harboring EGFR mutations [J]. Oncogene 40(2):355–368
37. WANG S, SHI J, YE Z et al (2019) Predicting EGFR mutation status in lung adenocarcinoma on computed tomography image using deep learning [J].Eur Respir J, 53(3)
38. SHIN SH, JEONG B H LEEH et al (2018) Anaplastic lymphoma kinase rearrangement in surgically resected stage IA lung adenocarcinoma [J]. J Thorac Dis 10(6):3460–3467
39. VANDERLAAN PA, RANGACHARI D, MOCKUS S M et al (2017) Mutations in TP53, PIK3CA, PTEN and other genes in EGFR mutated lung cancers: Correlation with clinical outcomes [J]. Lung Cancer 106:17–21
40. XU Y, TONG X (2018) Short-Term Responders of Non-Small Cell Lung Cancer Patients to EGFR Tyrosine Kinase Inhibitors Display High Prevalence of TP53 Mutations and Primary Resistance Mechanisms [J]. Transl Oncol 11(6):1364–1369
41. PROS E, SAIGI M (2020) ALAMEDA D, et al. Genome-wide profiling of non-smoking-related lung cancer cells reveals common RB1 rearrangements associated with histopathologic transformation in

EGFR-mutant tumors [J], vol 31. ANNALS OF ONCOLOGY, pp 274–2822

42. WANG PENGS, ZHANG R (2019) EGFR-TKI resistance promotes immune escape in lung cancer via increased PD-L1 expression [J]. Mol Cancer 18(1):165
43. POSTOW M A, CALLAHAN M K, WOLCHOK JD (2015) Immune Checkpoint Blockade in Cancer Therapy [J]. J Clin Oncol 33(17):1974–1982
44. RITTMEYER A, BARLESI F (2017) Atezolizumab versus docetaxel in patients with previously treated non-small-cell lung cancer (OAK): a phase 3, open-label, multicentre randomised controlled trial [J]. The Lancet 389(10066):255–265
45. ANTONIA SJ, VILLEGAS A (2018) Overall Survival with Durvalumab after Chemoradiotherapy in Stage III NSCLC [J]. N Engl J Med 379(24):2342–2350
46. MOK T S K, WU Y-L, KUDABA I et al (2019) Pembrolizumab versus chemotherapy for previously untreated, PD-L1-expressing, locally advanced or metastatic non-small-cell lung cancer (KEYNOTE-042): a randomised, open-label, controlled, phase 3 trial [J]. The Lancet 393(10183):1819–1830
47. ZHOU Y, ZHANG Y, GUO G et al (2020) Nivolumab plus ipilimumab versus pembrolizumab as chemotherapy-free, first-line treatment for PD-L1-positive non-small cell lung cancer [J]. Clin Transl Med 10(1):107–115
48. SUDA K, SHIMOJI M (2019) SHIMIZU S, Comparison of PD-L1 Expression Status between Pure-Solid Versus Part-Solid Lung Adenocarcinomas [J].Biomolecules, 9(9)
49. CARBONE D P, RECK M, PAZ-ARES L et al (2017) First-Line Nivolumab in Stage IV or Recurrent Non-Small-Cell Lung Cancer [J]. N Engl J Med 376(25):2415–2426
50. DONG Z Y SUS, XIE Z et al (2018) Strong Programmed Death Ligand 1 Expression Predicts Poor Response and De Novo Resistance to EGFR Tyrosine Kinase Inhibitors Among NSCLC Patients With EGFR Mutation [J]. J Thorac Oncol 13(11):1668–1675
51. BITON J, MANSUET-LUPO A, PECUCHET N et al (2018) TP53, STK11, and EGFR Mutations Predict Tumor Immune Profile and the Response to Anti-PD-1 in Lung Adenocarcinoma [J]. Clin Cancer Res 24(22):5710–5723
52. PLANCHARD D, YOKOI T, MCCLEOD M J et al (2016) A Phase III Study of Durvalumab (MEDI4736) With or Without Tremelimumab for Previously Treated Patients With Advanced NSCLC: Rationale and Protocol Design of the ARCTIC Study [J]. Clin Lung Cancer 17(3):232–6e1
53. HELLMANN MD, NATHANSON T, RIZVI H et al (2018) Genomic Features of Response to Combination Immunotherapy in Patients with Advanced Non-Small-Cell Lung Cancer [J]. Cancer Cell 33(5):843–852e4
54. RIZVI N A, HELLMANN M D SNYDERA et al (2015) Cancer immunology. Mutational landscape determines sensitivity to PD-1 blockade in non-small cell lung cancer [J]. Science 348(6230):124–128
55. SNYDER A, MAKAROV V, MERGHOUB T et al (2014) Genetic basis for clinical response to CTLA-4 blockade in melanoma [J]. N Engl J Med 371(23):2189–2199

56. WU Y L, TSUBOI M, HE J et al (2020) Osimertinib in Resected EGFR-Mutated Non-Small-Cell Lung Cancer [J]. N Engl J Med 383(18):1711–1723

57. **Statements and Declarations**

Tables

Table 1

Basic information of 328 patients with ground glass nodules

Basic clinical characters	Total	Percentage (%)
Gender		
male	106	32.3
female	222	67.7
Age		
≤45	42	12.8
45 to 65	228	69.5
≥65	58	17.7
Smoker		
ever	84	25.6
never	244	74.4
Number		
single	287	87.2
multiple	41	12.8
Pathological pattern		
AIS	26	6.9
MIA	128	33.9
IAC	224	59.2
Lymph node metastasis		
yes	5	1.5
no	323	98.5
Clinical stage		
IA	240	73.2
IB	80	24.4
IIA	2	0.6
IIB	5	1.5
IIIA	1	0.3

AIS, adenocarcinoma in situ; MIA, minimally invasive adenocarcinoma; IAC, invasive adenocarcinoma;

Table 2

Morphological and radiological characteristics of GGNs

GGN	Percentage (%)	AIS/MIA (n=154)	IAC (n=224)	p Value
Size [cm]	-	0.923±0.0298	1.773±0.0495	<0.001
CTR	-	0.13±0.027	0.57±0.033	<0.001
Location				0.720
LUL	27.2	38	65	
LLL	11.9	21	24	
RUL	37.8	57	86	
RML	8.2	15	16	
RLL	14.8	23	33	
Density				<0.001
pure	60.8	134	96	
mix	39.2	20	128	
Shape				<0.001
round	72.5	147	127	
irregular	27.5	7	97	
Bound				0.008
clear	38.1	71	73	
indistinct	61.9	83	151	
Lobulation				<0.001
yes	38.4	15	130	
no	61.6	139	94	
Spicule sign				<0.001
yes	13.0	3	46	
no	87.0	151	178	
Bubble lucency				<0.001
yes	49.7	40	148	
no	50.3	114	76	
Vessel gather				<0.001
yes	25.9	11	87	

no	74.1	143	137	
Air bronchogram				<0.001
yes	21.2	12	68	
no	78.8	142	156	
Pleural traction				<0.001
yes	32.8	16	108	
no	67.2	138	116	

AIS, adenocarcinoma in situ; MIA, minimally invasive adenocarcinoma; IAC, invasive adenocarcinoma; CTR, consolidation tumor ratio; LUL, left upper lobe; LLL, left lower lobe; RUL, right upper lobe; RML, right middle lobe; RLL, right lower lobe;

Table 3

Multivariate regression predictors analysis of GGNs

Factor	SE	Wald	95% CI	p-Value
Maximum diameter	0.451	34.917	5.946–34.888	<0.001
CTR	0.92	5.478	1.419–52.175	0.019
Lobulation	0.406	7.033	0.154–0.755	0.008
Pleural traction	0.374	6.703	0.183–0.791	0.01

SE, standard error; CI, confidence interval; CTR, consolidation tumor ratio;

Figures

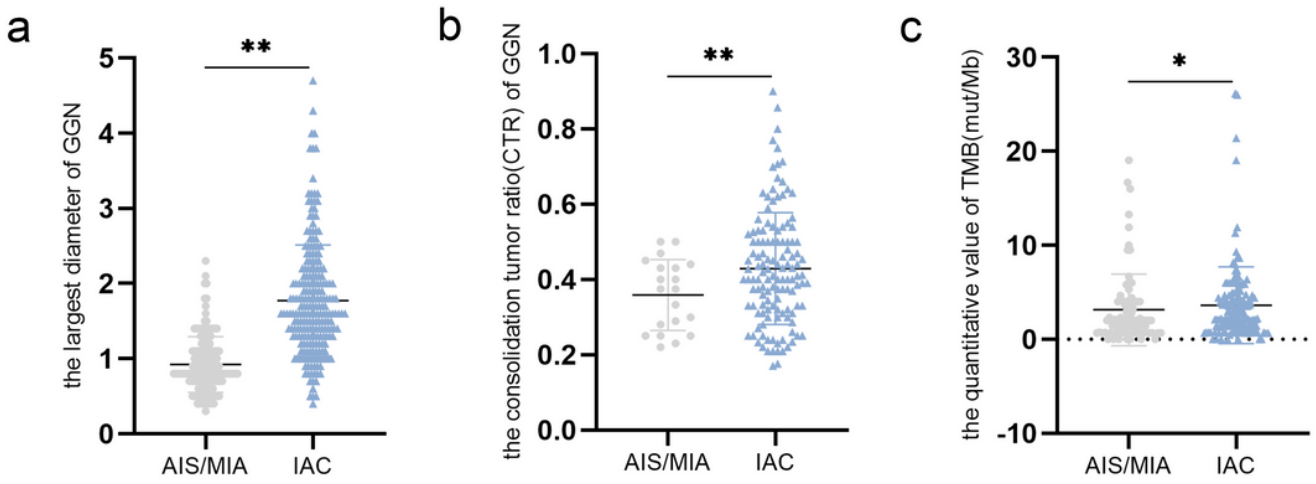

Figure 1

Comparisons of the quantitative indexes of the diameter, the consolidation tumor ratio (CTR), and tumor mutational burden (TMB) between pre-invasive adenocarcinoma (adenocarcinoma in situ [AIS] and minimally invasive adenocarcinoma [MIA]) and invasive adenocarcinoma (IAC) with pulmonary ground-glass nodules (GGNs). (a) GGNs of IAC have bigger size of diameter than GGNs of AIS/MIA. (b) GGNs of IAC possess more solid components than GGNs of AIS/MIA. (c) The value of TMB in group of IAC has a little bit higher than AIS/MIA. * $p < 0.05$.

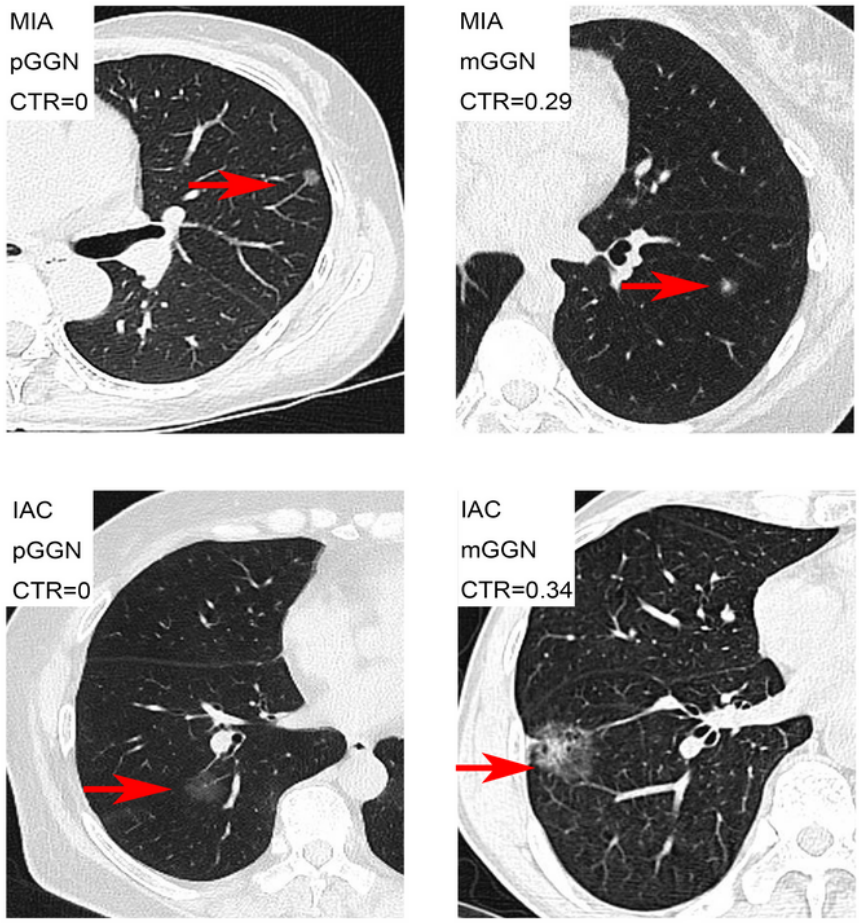

Figure 2

Basic morphology performances of pure ground-glass nodules (pGGNs) and mixed ground-glass nodules (mGGNs) are showed with different value of CTR in MIA and IAC, respectively. Arrows indicate GGNs.

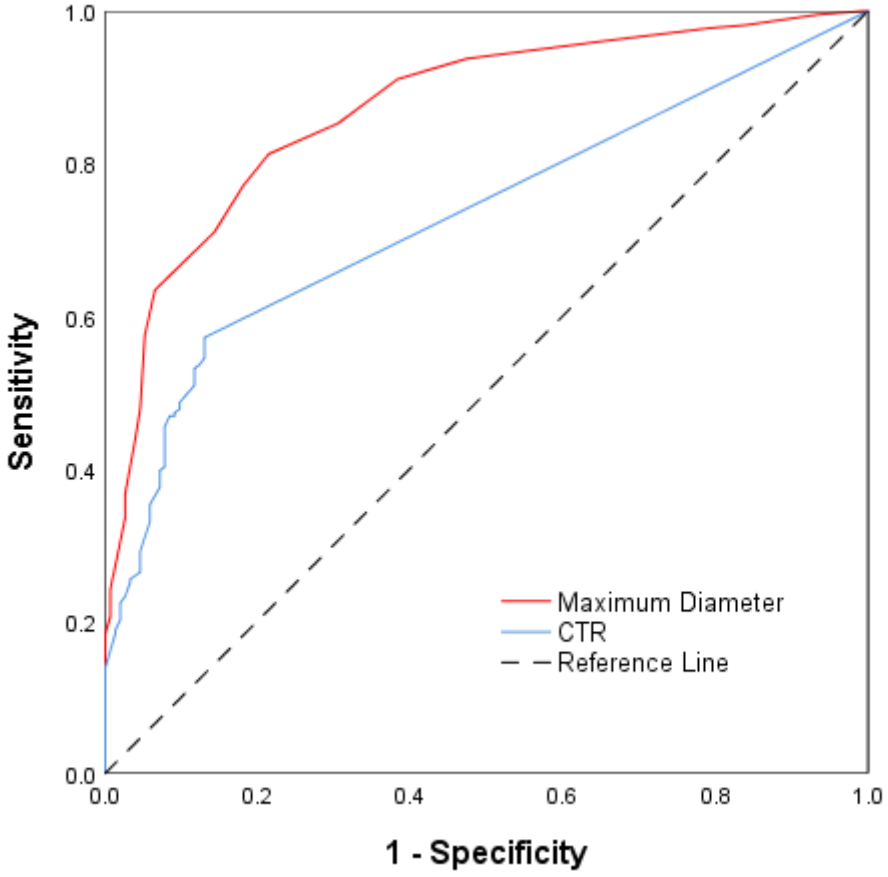

Figure 3

The receiver operating characteristic curve (ROC) and the area under the curve (AUC) of nodule diameter and consolidation tumor ratio are showed to better diagnose pre-invasive and invasive adenocarcinoma with best sensitivity and specificity. The maximum diameter is a comprehensive index to apply in clinical activity, while CTR has more accurate specificity.

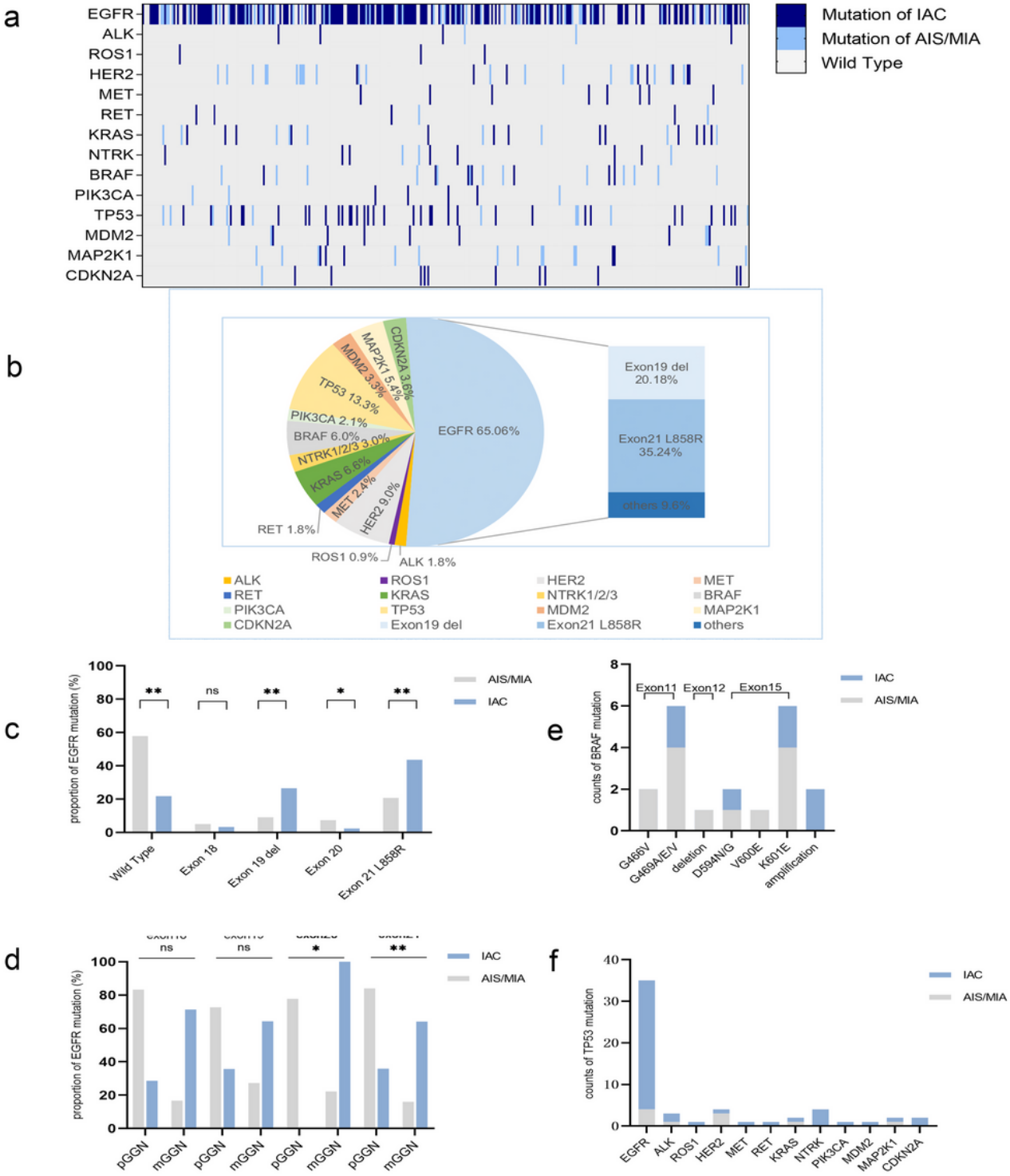

Figure 4

Comparison of relative gene mutations in pulmonary GGNs from lung cancer samples. (a) The distribution of relative gene mutations in pre-invasive and invasive adenocarcinoma. (b) A pie chart illustrating the proportion of mutated genes in lung cancer GGNs. (c) The difference between the most common mutation sites of EGFR in two groups of GGN pathological subtypes. (d) The distribution of

pGGNs and mGGNs in common EGFR mutations. (e) Diverse site changes occur in gene BRAF mutations. (f) Levels of TP53 inactivation following various gene mutations.

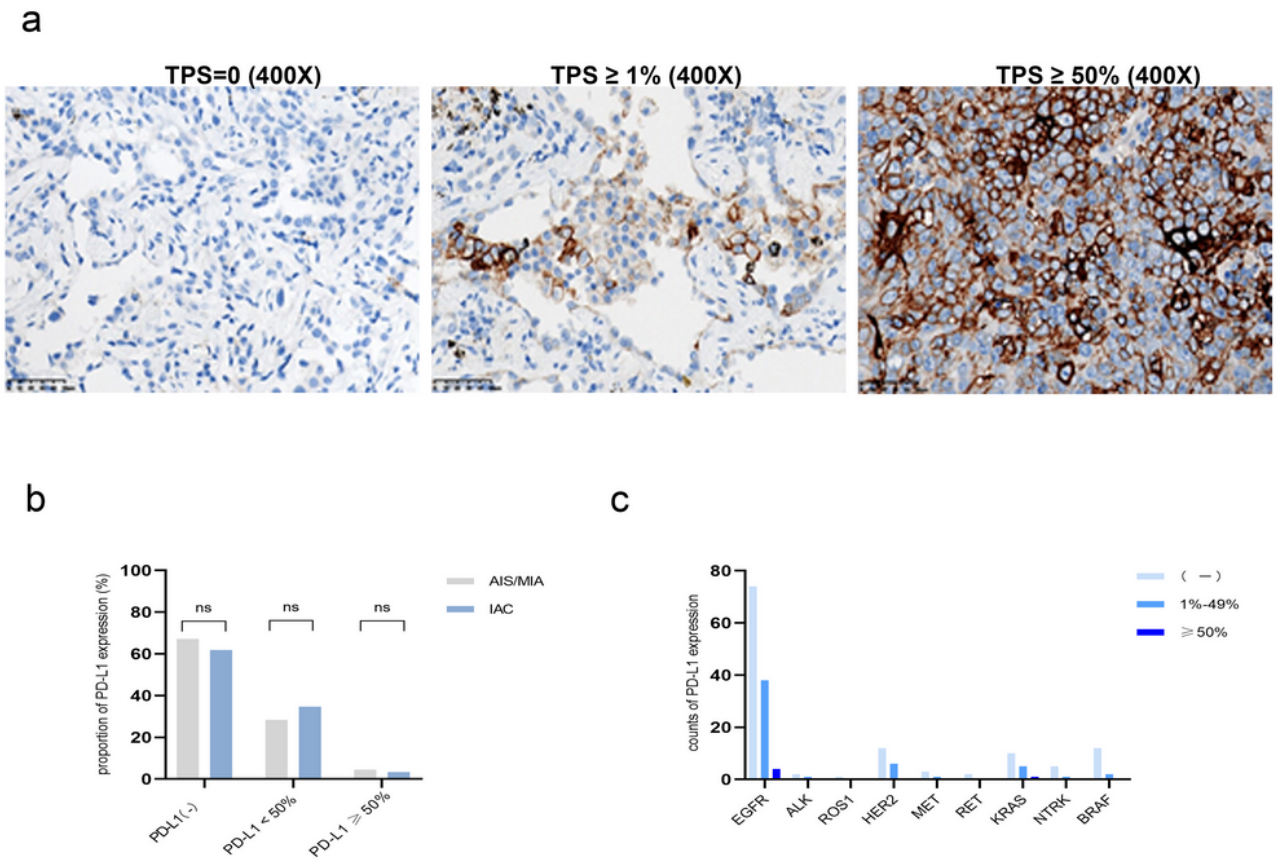

Figure 5

Comparison of programmed death ligand 1 (PD-L1) expression levels in lung cancer tissues. (a) The PD-L1 protein was detected by immunohistochemistry staining and showed negative as well as positive expression with three degrees of tumor proportion score (TPS); scale bars, 50μm. (b) The distribution of

PD-L1 expression in pre-invasive and invasive adenocarcinoma. (c) The distribution of three expression levels of PD-L1 in tissues with diverse gene mutations.